John Innes Centre
Unlocking Nature's Diversity

CAMBRIDGE
UNIVERSITY PRESS

Temporal and spatial auxin responsive networks in maize primary roots

Maxwell R. McReynolds[1], Linkan Dash[2], Christian Montes[1], Melissa A. Draves[2], Michelle G. Lang[2,3], Justin W. Walley[1] and Dior R. Kelley[2]

[1]Department of Plant Pathology and Microbiology, Iowa State University, Ames, Iowa 50011, USA; [2]Department of Genetics, Development and Cell Biology, Iowa State University, Ames, Iowa 50011, USA; [3]Corteva Agriscience, Johnston, Iowa 50131, USA

Abstract

Auxin is a key regulator of root morphogenesis across angiosperms. To better understand auxin-regulated networks underlying maize root development, we have characterized auxin-responsive transcription across two time points (30 and 120 min) and four regions of the primary root: the meristematic zone, elongation zone, cortex and stele. Hundreds of auxin-regulated genes involved in diverse biological processes were quantified in these different root regions. In general, most auxin-regulated genes are region unique and are predominantly observed in differentiated tissues compared with the root meristem. Auxin gene regulatory networks were reconstructed with these data to identify key transcription factors that may underlie auxin responses in maize roots. Additionally, Auxin-Response Factor subnetworks were generated to identify target genes that exhibit tissue or temporal specificity in response to auxin. These networks describe novel molecular connections underlying maize root development and provide a foundation for functional genomic studies in a key crop.

1. Introduction

Auxin is a central regulator of root development, playing critical roles in processes such as meristem maintenance and lateral root formation (reviewed in Atkinson et al., 2014). Root architecture varies among angiosperms and can be influenced by both nutrient and hormone signaling (Hochholdinger et al., 2018; Liu & von Wirén, 2022). The current models for auxin perception and signaling encompass decades of studies (Powers & Strader, 2020). Nuclear auxin perception occurs via a co-receptor complex composed of evolutionarily conserved F-box TRANSPORT INHIBITOR RESPONSE1/AUXIN SIGNALING F-BOX (TIR1/AFB) and AUXIN/INDOLE ACETIC ACID (Aux/IAA) proteins (Calderón Villalobos et al., 2012; Dharmasiri et al., 2005; Kepinski & Leyser, 2004). Because TIR1/AFB proteins encode E3 ubiquitin ligase enzymes, this interaction leads to ubiquitination and degradation of Aux/IAA proteins (Kelley, 2018). Additionally, Aux/IAA proteins (29 family members in Arabidopsis and 31 in maize) are transcriptional repressors that actively repress AUXIN RESPONSE FACTOR (ARF) transcription factors in cooperation with the TOPLESS co-repressor family of proteins (Gallavotti et al., 2010; Szemenyei et al., 2008). Thus, in the absence of Aux/IAA proteins ARF transcription factors are able to transcriptionally regulate gene expression very rapidly. The ARF protein family (23 members in Arabidopsis and 31–36 members in maize) has been recently divided into three classes based on their structure and ability to either activate or repress gene expression (termed "activators" or "repressors") (Galli et al., 2018; Mutte et al., 2018).

Auxin-responsive gene expression in primary roots has been studied in Arabidopsis (Bargmann et al., 2013; Lewis et al., 2013; Nemhauser et al., 2006; Pu et al., 2019) and maize (Galli et al., 2018; Ravazzolo et al., 2021; Wang et al., 2021; Xing et al., 2011). While maize root systems differ considerably in their anatomy and architecture from Arabidopsis roots (Hochholdinger et al., 2018; Hochholdinger & Zimmermann, 2008), there are a couple maize root mutants that have been linked to auxin either directly or indirectly, highlighting the central role that auxin plays in root development. For example, *rootless undetectable meristem 1* (*rum1*) encodes an

Aux/IAA protein that is required for embryonic and postembryonic root formation (von Behrens et al., 2011). In addition, the *rootless concerning crown and seminal roots* (*rtcs*) mutant encodes a LATERAL ORGAN BOUNDARY (LOB) transcription factor which is linked to auxin-regulated gene expression (Taramino et al., 2007; Xu et al., 2015).

Given that root system development differs between maize and Arabidopsis (Hochholdinger, 2009; Hochholdinger & Zimmermann, 2008) and that auxin responses are known to be influenced by cellular context (Bargmann et al., 2013; Brunoud et al., 2012; Novák et al., 2012; Truskina et al., 2021), an increased resolution of auxin-mediated transcription in maize would be beneficial. The primary maize root is divided into three key developmental regions: the meristematic zone, the elongation zone and the maturation zone with specialized functions (Hochholdinger, 2009; Hochholdinger et al., 2018). The meristematic zone includes the distal tip of the primary root and is composed stem cells and the lateral root cap (Hochholdinger, 2009). While the lateral root cap provides protection and gravity perception (Matsuyama et al., 1999), the meristem functions to sustain root organogenesis via a balance of self-renewal and differentiation (Jiang et al., 2010). The elongation zone is composed of differentiating root cells that are required for gravitropism and sensitive to exogenous auxin treatment (Ishikawa & Evans, 1993). Terminally differentiated cells, such as root hairs and tracheids, are found within the maturation zone and thus represent a high degree of complexity due to their myriad of functions (Hochholdinger, 2009). A high-resolution map of gene expression across these regions of the root has revealed extensive tissue specificity and plasticity (Marcon et al., 2015).

An outstanding question in the field is how auxin-responsive gene expression is incorporated into maize root development. In this study, we profiled auxin-responsive gene expression with spatial and temporal resolution to further our understanding of how auxin influences transcriptional responses in maize roots. Specifically, we performed transcriptome analysis of the meristematic zone, elongation zone, cortex, and stele of 5-day-old primary maize roots following 30 and 120 min of exogenous indole-3-acetic acid treatment. This analysis demonstrates that auxin-responsive gene expression in roots exhibits both tissue and temporal specificity.

Biological networks can describe molecular connections underlying cellular processes and provide insight towards complex phenomena (Haque et al., 2019; Marshall-Colón & Kliebenstein, 2019; Walley et al., 2016). With respect to auxin signaling, several aspects of auxin action are well-suited to network analyses. For instance, the direct influence of auxin on transcription can be modeled through the reconstruction of gene regulatory networks (GRNs) that can be used to infer the structure of gene expression programs that underpin development. Using the auxin transcriptome data generated herein we generated novel auxin-dependent predictive GRNs that underlie maize root morphogenesis. These data expand our understanding of shared and unique properties of maize ARF transcription factors, identify key auxin marker genes in maize roots, and quantify auxin-regulated transcription across the developing maize root to inform further research on crop root development.

2. Methods

2.1. Plant material

Zea mays inbred B73 kernels were surface sterilized in 5% bleach for 15 min and rinsed three times with sterile deionized water. For every 10 kernels, three pieces of seed germination paper (Anchor Paper Company, 10 × 15 L 38# regular weight seed germination paper) were soaked in a solution of freshly prepared Captan fungicide (2.5 g/L). Ten kernels were placed ~5 cm from the top of the paper in the middle sheet, covered with the top sheet, and rolled into a cylinder lengthwise using the rolled towel method (Hochholdinger, 2009). Twelve paper rolls were placed in a 4 L Nalgene beaker containing 400 mL of 0.5X Linsmaier and Skoog (LS) (2.4 g/L) pH buffered basal salts (Caisson Labs). The rolled towels were placed in a Percival growth chamber set to 22ºC, long day (16 hr light, 8 hr dark) white light at 160 μmol·m^{-2}s^{-1} light intensity. After 2 days the rolls were opened and the seeds were scored for germination. Any ungerminated kernels were removed and this was designated day one. After 2 days of growth the liquid media was poured off and replaced with fresh 400 mL of 0.5X LS. Five days after germination (5 DAG) the seedlings were removed from the towels prior to mock or auxin treatments followed by dissection.

2.2. Auxin treatments

10 mM Indole-3-acetic acid (IAA) stocks were prepared in 95% ethanol and stored at $-20°$C. Immediately before performing the auxin treatments, one liter of 10 μM IAA was prepared by diluting the 10 mM stock 1:1,000 into 0.5X LS media, resulting in a final concentration of 0.095% ethanol. As a corresponding "mock" control, one liter of 0.095% ethanol was prepared by diluting 95% ethanol 1:1,000. Seedlings were placed in 0.5X LS supplemented with 10 μM IAA ("auxin" treatment) or 0.095% ethanol ("mock" control) and incubated at room temperature for 30 and 120 min. For each biological replicate, 30–80 primary roots (approximately 2–4 cm in length) were hand dissected into meristematic zone, elongation zone, cortical parenchyma and epidermis (referred to as "cortex" hereafter), and stele according to previous methods (Marcon et al., 2015; Saleem et al., 2010; Walley et al., 2016) to yield at least 100 mg of tissue per sample and replicate. Total tissue weights per tissue replicate varied from 100–600 mg. In total, three biological replicates were collected for each tissue and time point for the transcriptome analysis. Tissues were immediately flash frozen in liquid nitrogen and stored at $-80°$C until all replicates were harvested.

2.3. RNA extraction and transcriptome sequencing

Root tissues (100–500 mg per sample) were ground to fine powder in liquid nitrogen using a pre-chilled mortar and pestle. RNA was extracted from ~100 mg of tissue using Trizol (Invitrogen) and further purified using Qiagen RNeasy kit with on column DNase treatment (Walley et al., 2010). Isolated RNA concentration and quality were checked using a Nanodrop, Qubit, and Bioanalyzer. Total RNA was used to generate QuantSeq 3'mRNA libraries using a Lexogen 3$'$ mRNA-Seq FWD kit and 48 unique indices (Moll et al., 2014). Libraries were run on an Illumina HiSeq 3,000 to generate 100 bp single-end (SE) reads.

2.4. RNA-seq analysis

FASTQ sequence files were deposited at the NCBI Sequence Read Archive (BioProject accession number PRJNA791716). Files were checked via FASTQC to obtain sequence quality information. The FASTQ files were then run through the following bioinformatic pipeline as suggested by Lexogen. First, adapters

and low-quality tails were removed using *bbduk* from the BBTools suite (sourceforge.net/projects/bbmap/). Alignment to the B73 v4 genome (Jiao et al., 2017) was performed using STAR (Dobin et al., 2013) and indexing was executed using SAMTools (Li et al., 2009). HTSeq (Anders et al., 2015) was used to generate count files which were then analyzed via PoissonSeq (Li et al., 2012). Differentially expressed (DE) genes were identified between mock and time-matched treated samples in each tissue using a false discovery rate (FDR; adjusted *p*-value) of $q < 0.1$.

2.5. Gene regulatory network analysis

Transcription factor-centered GRNs were generated using Spatiotemporal Clustering and Inference of Omics Networks (SC-ION) version 2.1 (Clark et al., 2021). For clustering and network reconstruction within SC-ION, a trimmed mean of M values (TMM)-normalized counts matrix of all detected transcripts across all samples from the RNA-seq analysis was selected as the input file for both the target matrix and regulator matrix. To specify network candidate targets, a list of gene IDs corresponding to PoissonSeq-derived significant DE genes ($q < 0.1$) from comparisons between tissue types or in IAA versus mock treatments was used as the target list. Similarly, to classify candidate regulators, IDs of significant DE genes from the comparisons between tissue types or in IAA versus mock treatments, which were annotated as TFs according to Grassius (Yilmaz et al., 2009) were used as the regulator list. Non-temporal clustering via Independent Component Analysis (ICA) (Nascimento et al., 2017) was selected and SC-ION was supplied a matrix consisting of TMM-normalized counts of transcripts averaged across biological replicate for each tissue type at 30 min. GRNs for each ICA cluster were then inferred using SC-ION's implementation of the random forest algorithm, GENIE3 (Huynh-Thu et al., 2010). The SC-ION output table consisting of predicted regulator-target interactions as well as a numeric "weight" value for each pair indicating the confidence of their connection was imported into Cytoscape (Shannon et al., 2003) for GRN visualization. For the spatiotemporal GRN, the nodes (genes) were colored in Cytoscape according to their temporal IAA responsiveness (i.e., up or down at 30 or 120 min) and grouped by tissue cluster enrichment. To visualize the ARF transcription factor subnetworks, ARF-specific regulators and their first-neighbor targets were extracted from the SC-ION output table and imported into Cytoscape. The grouping of ARFs by clade membership and coloring of ARF nodes and their first neighbor targets was done within Cytoscape.

2.6. Gene ontology enrichment and UpSet analyses

Gene ontology (GO) enrichment analysis was performed using the *Zea mays* B73 inbred reference genome in PANTHER. A Fisher's exact test type and an FDR correction using the Benjamini–Hochberg method with a cutoff of 0.05 was used to identify significantly enriched GO terms. Significant GO biological process terms were plotted on the y-axis against their genotype/treatments on the *x*-axis using multidimensional dot plots (Bonnot et al., 2019). UpSet plots were generated using the UpsetR package in RStudio and ordered by frequency (Conway et al., 2017). The "nintersects" argument was used to output the 20 (Figure 2 and Supplemental Figure S2) and 50 (Supplemental Figure S3) most populated intersections. Additional code was written to extract gene identifiers among shared lists of differentially expressed genes within an UpSet plot; data processing scripts are available

from a GitHub repository: https://github.com/mmcreyno92/AuxinRootAtlas.

2.7. Hierarchical clustering and visualization by heatmaps

Hierarchical clustering of transcript abundance was independently performed in each tissue on genes that were DE in response to auxin and plotted as heatmaps using the Morpheus software from the Broad Institute (https://software.broadinstitute.org/morpheus/). The heatmaps show the row normalized transcript level. Row normalization was done by converting to *Z*-scores using the "subtracted by row mean and divided by row standard deviation" adjustment.

3. Results and discussion

3.1. Auxin responsive transcriptome profiles in primary maize roots across space and time

Maize root growth and development have been linked to auxin using hormone application essays (Pilet & Saugy, 1985) and genetic studies (von Behrens et al., 2011; Zhang et al., 2015; 2016). In Arabidopsis, the transcriptional responses of root cells to auxin have been characterized (Bargmann et al., 2013) and provide foundational knowledge of how auxin impacts gene expression in a context-dependent manner. In maize, auxin-responsive gene expression has been characterized on whole seedlings (Galli et al., 2018), but auxin-driven gene expression patterns within the root are not well understood. The overall goal of this study was to characterize the auxin-responsive transcriptome within maize primary roots across four key cellular regions: the meristematic zone, elongation zone, and the cortex and stele within the differentiation zone (Marcon et al., 2015; Paschold et al., 2014; Walley et al., 2016) to determine how auxin can impact gene expression in roots (Figure 1a). Five-day-old B73 maize primary roots were treated with 10 μM IAA ("auxin") or 0.095% ethanol ("mock" solvent control) for 30 and 120 min and then dissected into four regions (Figure 1a). This concentration of auxin was selected based on previous work that demonstrated auxin-dependent degradation of an Aux/IAA-based fluorescence reporter (DII-VENUS) occurred rapidly following 10 μM IAA treatments (Mir et al., 2017) and can lead to primary root inhibition (Supplemental Figure S1). These treatments were performed for 30 and 120 min in order to capture the temporal nature of auxin signaling, given that transcriptional response and Aux/IAA turnover occur rapidly within these timeframes of hormone exposure (Bargmann et al., 2013; Mir et al., 2017; Zhang et al., 2016). Transcriptome profiling was performed on these tissues using the 3' QuantSeq method with three biological replicates for each tissue/treatment/time. From this analysis, we identified 32,832 distinct transcripts in total across all tissues. Within the meristematic zone, relatively few auxin-responsive genes were observed (Figure 1b Supplemental Table S1). In contrast, hundreds of genes were induced or repressed following auxin treatment within the elongation zone, cortex, and stele. This result suggests that meristematic zone cells may be less sensitive to exogenous auxin effects, as endogenous levels of IAA are already high in this region of the root (Mir et al., 2017; Pilet & Saugy, 1985). In addition, many of the observed auxin-regulated genes include *AUXIN INDOLE-3-ACETIC ACID INDUCIBLE* (*Aux/IAA*), *GRETCHEN HAGEN* (*GH*), *SMALL AUXIN UPREGULATED* (*SAUR*), and *LATERAL BOUNDARY DOMAIN* (*LBD*) family members, which is consistent with previous studies on auxin-
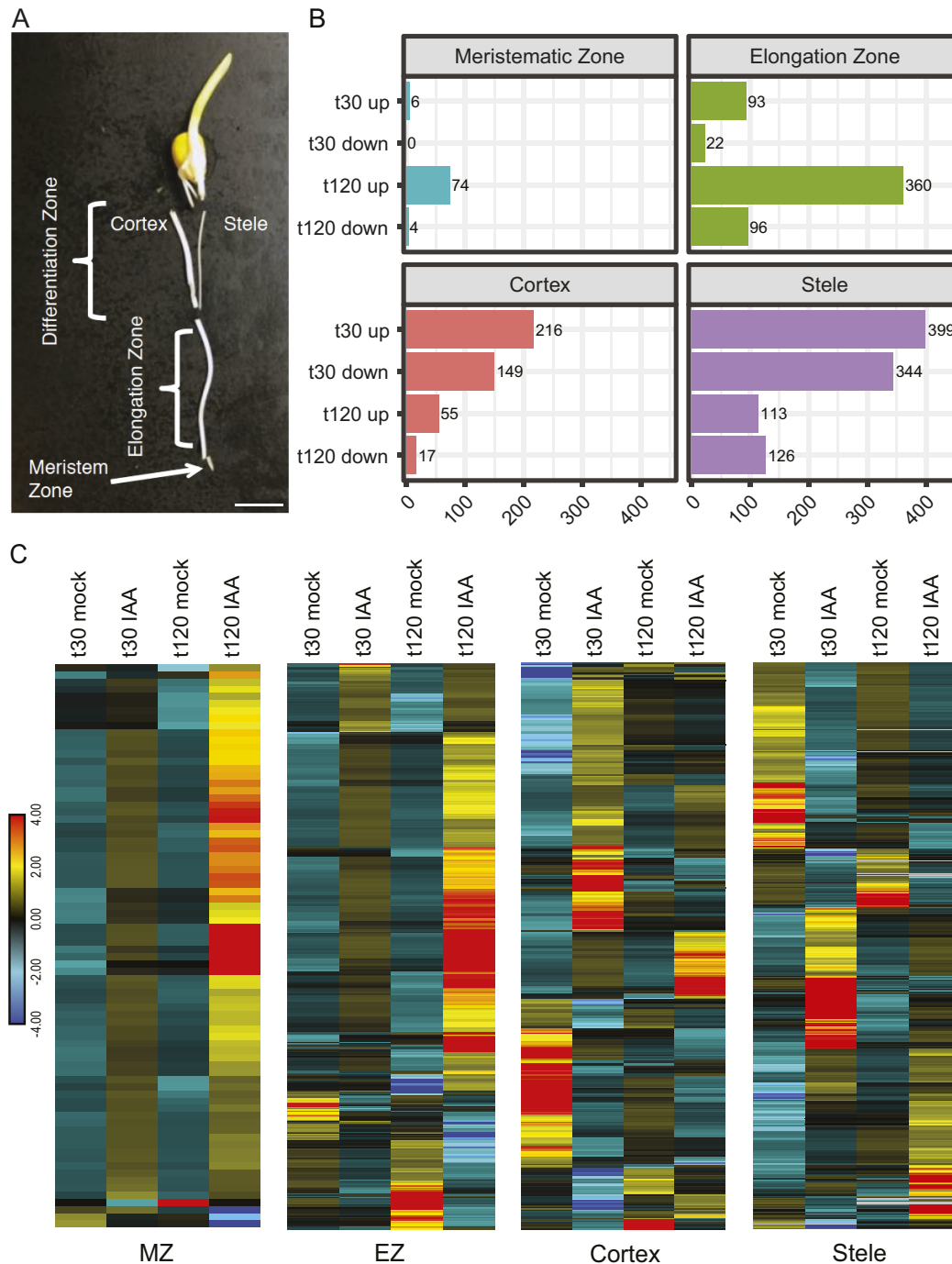
Fig. 1. Identification of auxin-responsive genes across four key regions of the primary maize root. (a) Picture of maize primary dissected root regions profiled in this study. Five-day-old primary maize roots were dissected into the four regions indicated. The distal 2 mm of the root tip corresponds to the meristematic zone (MZ). The elongation zone (EZ) is the proximal zone adjacent to the MZ root tip up to where the root hairs emerge. The differentiation zone, starting with the root hair zone, was mechanically separated into cortex (C) and stele (S) by snapping the root from the kernel and pulling the stele out from the cortex. Scale bar = 1 cm. (b) Differentially expressed genes within each root region at 30 min (t30) and 120 min (t120) were identified by comparing 10 □M indole-3-acetic acid (auxin) treated samples to mock-treated samples at *q* < 0.1. The *x*-axes represent the number of DE genes. (c) Heatmaps ordered by hierarchical clustering of the genes that are DE in response to auxin within each tissue profiled. Hierarchical clustering was independently carried out within each tissue.

mediated gene expression from Arabidopsis roots (Bargmann et al., 2013; Lewis et al., 2013). In Arabidopsis roots, early up-regulated clusters of co-expressed genes are enriched with these same auxin-response annotations (Lewis et al., 2013), which is consistent with the temporal effects observed here.

Within the cortex and stele more auxin-regulated genes are observed at 30 min compared with 120 min. In contrast, within the elongation zone, we observed more up-regulated genes at 120 min compared with 30 min. These patterns may reflect the altered chromatin state or transcription factor properties associated with cellular state as cortex and stele cells are further differentiated compared with elongation zone cells. A previous time course of auxin-responsive gene expression in Arabidopsis roots identified few transcriptional changes at 30 min and a marked bimodal
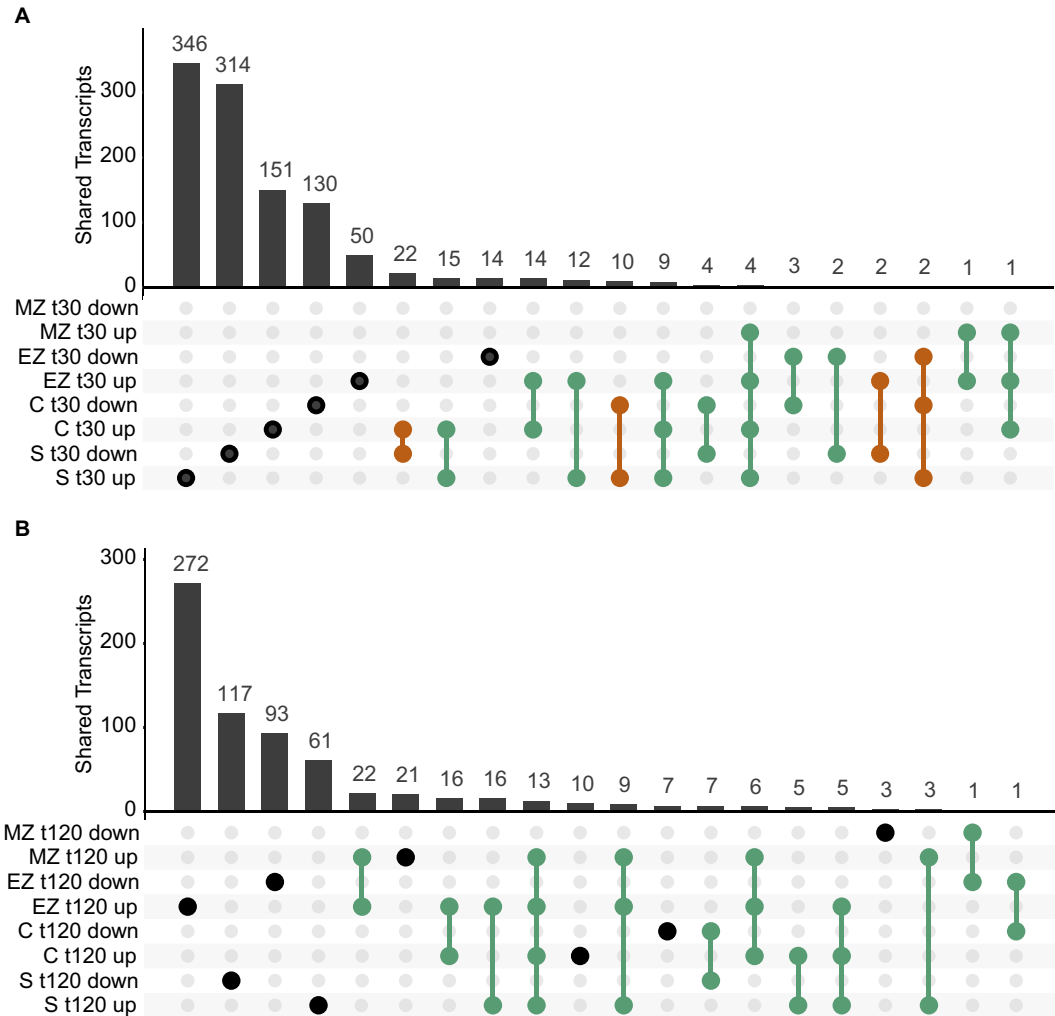
Fig. 2. A comparison of differentially expressed genes in maize roots across four regions at two different time points in response to auxin. (a) UpSet plot of differentially expressed transcripts at 30 min (t30). (b) UpSet plot of auxin-responsive DE transcripts at 120 min (t120). Concordant and discordant comparisons are indicated in green and vermillion, respectively. Only the top 20 most populated intersections are visualized. Abbreviations: auxin, indole-3-acetic acid treatment compared with mock treatment; C, cortex; EZ, elongation zone; MZ, meristematic zone; S, stele, auxin.

distribution at 120 min (2 hr) (Lewis et al., 2013), which is consistent with this study.

3.2. Auxin-regulated gene expression in maize primary roots is region specific

Auxin-mediated gene expression is context dependent. To examine shared and uniquely regulated transcripts across the four sampled root regions we generated UpSet plots comparing auxin-responsive transcripts within each time point (Figure 2 and Supplemental Figure S2) as well as DE between tissues (Supplemental Figure S3). Given that there are numerous possible comparisons with four regions and two categories of DE (up or down) we selected the top 20 comparisons for visualization. At both 30 and 120 min after auxin treatment, relative to mock treatment, the majority of the observed DE genes are region specific. At 30 min after treatment auxin up- and down-regulated genes across regions include both concordant and discordant properties. For example, there are 22 genes that are up-regulated in the cortex at 30 min after auxin treatment that are down-regulated in the stele (Figure 2a). Thus, these transcripts are considered to be discordant because they

display opposite expression patterns between neighboring tissues. In contrast, at 120 min after treatment, the observed DE genes in common between tissues are only concordant. For example, all shared transcripts between tissues at this timepoint display the same direction of expression across tissues. This result suggests that early auxin-mediated transcriptional changes may include both repression and activation at the same genes in a tissue-specific manner, while later effects (i.e., 120 min) of auxin may uniformly influence suites of genes irrespective of cellular context.

These comparisons provide the opportunity to identify robust auxin-responsive transcripts which are up-regulated irrespective of tissue or time point. For example, there are four transcripts that are auxin induced in the meristematic zone, elongation zone, cortex, and stele at 30 min and 13 such transcripts at 120 min. These transcripts include *AUX/IAA-transcription factor 22* (*IAA22/ Zm00001d013707*), *Aux/IAA24* (*Zm00001d018414*), *DIOXYGE-NASE FOR AUXIN OXIDATION 1* (*DAO1/Zm00001d003311*) and *AUXIN AMIDO SYNTHETASE2* (*AAS2/Zm00001d006753*). Notably, these are all encoded by genes with annotated functions as auxin transcriptional repressors and enzymes that conjugate or degrade IAA. Thus, these upregulated genes may reflect pathway
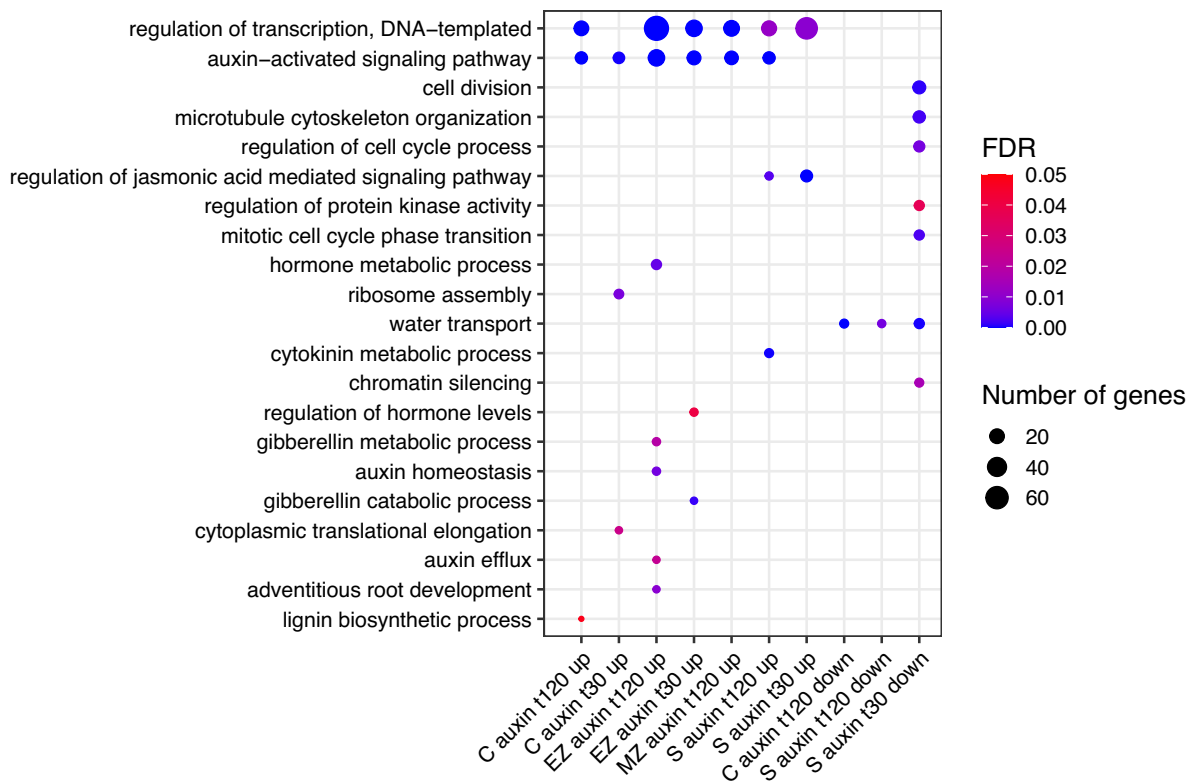
Fig. 3. Auxin-responsive genes between root regions are enriched in several gene ontology (GO) terms related to biological processes. Significant GO terms of interest in auxin down-regulated genes ("down") and auxin up-regulated genes ("up") are indicated on the y-axis. Only tissues with enriched GO terms are shown. False discovery rate (FDR) is color-coded from blue (0.00) to red (0.05). Size of the dot indicates the number of enriched genes within each GO term. Abbreviations: C, cortex; EZ, elongation zone; MZ, meristematic zone; S, stele, t30 = 30 min, t120 = 120 min.

feedback. From this analysis, a set of auxin-responsive marker genes have now been identified which can facilitate future studies on auxin signaling in maize roots.

3.3. Distinct biological processes are enriched among auxin-regulated genes across root regions

To determine if particular biological processes are auxin-regulated in root regions we performed a GO enrichment analysis. Many of the observed enriched GO terms are congruent with a previous study that examined the transcriptome profile of these root zones in the absence of treatment (Paschold et al., 2014), but we also identified a number of novel GO terms associated with hormone signaling, cell cycle, and gene regulation (Figure 3, Supplemental Figure S4, Supplemental Table S2). In general, auxin-induced genes are associated with transcription, auxin-activated signaling pathway, and gibberellin metabolism. In contrast, auxin repressed genes are associated with cell cycle, cell division, and chromatin silencing. Specifically, several Cyclins that promote cell cycle progression are repressed in the stele following a 30 min auxin treatment (Figure 3 and Supplemental Table S2), which is in line with a previous study linking low levels of auxin signaling with cell cycle progression (Mir et al., 2017).

In addition, we examined GO term enrichment between root regions to uncover tissue-specific processes that may underlie root structure (Supplemental Figure S4). In general, most GO terms appear to be tissue specific and many of the observed enriched GO terms are congruent with the previous study (Paschold et al., 2014). A couple of enriched GO terms stand out among the many

observed. First, transcripts involved in protein phosphorylation are more abundant in the stele compared with the meristem or the neighboring cortex. Another GO term observed across several tissue comparisons is 'microtubule-based movement', which is to be expected for cells undergoing cell elongation and/or differentiation. Secondary cell wall biogenesis is more prevalent in elongation zone expressed genes compared with meristem zone transcripts, which fits with our current understanding of cell wall composition across the primary root whereby secondary cell walls can be laid down in the elongation zone (Kozlova et al., 2020; Somssich et al., 2016). A comparison of the tissue-specific observed enriched GO terms across maize root tissues to the Bargmann et al. (2013) auxin cell-type specific study identified some shared terms, related to auxin signaling and cell wall. Specifically, we observed *cell wall organization* and *auxin-activated signaling pathway* terms enriched in auxin up-regulated genes in the stele compared with other tissues (Supplemental Figure S4) which is consistent with stele-associated terms observed in Arabidopsis (Bargmann et al., 2013). Altogether these results support the notion that root tissues exhibit unique cellular processes that may be linked to function.

3.4. Identification of spatially distinct auxin gene regulatory networks within primary roots

To infer regulatory relationships between auxin-responsive root transcription factors and their targets we generated a GRN. To reconstruct the predictive GRN we implemented our network inference pipeline, SC-ION, which is an extension of RTP-STAR and has been shown previously to successfully identify novel
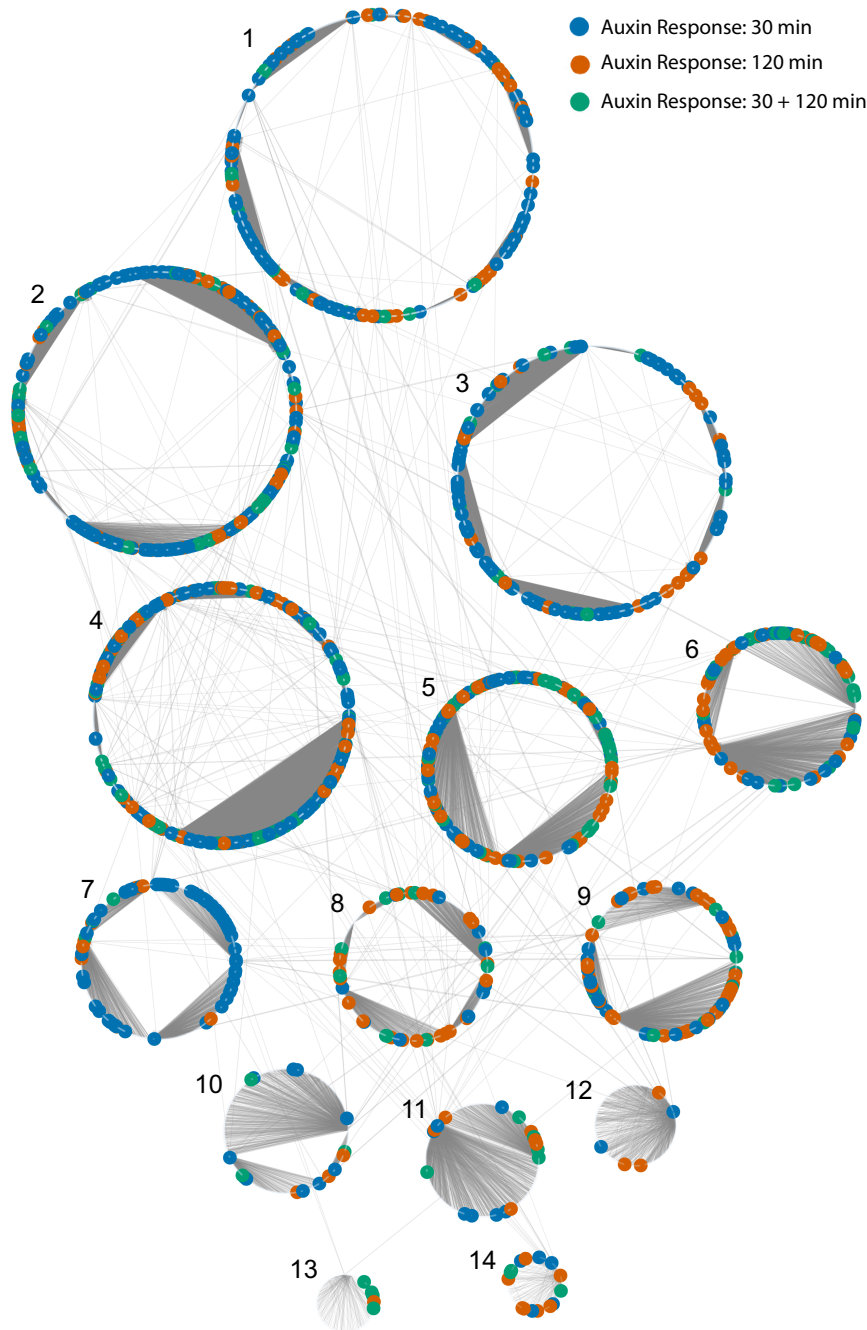
Fig. 4. A spatiotemporal auxin-responsive gene regulatory network in maize primary roots. The nodes (genes) are arranged in numbered circles to represent groupings of nodes (genes) that clustered together and were enriched within the same tissues. Colored nodes represent genes that are differentially expressed following auxin treatment. The temporal response to auxin is indicated by node color: blue, auxin responsive at 30 min; vermillion, auxin responsive at 120 min; and green, auxin responsive at both time points sampled. Each circular node represents a distinct cluster based on tissue: 1 = C + S, 2 = C, 3 = MZ, 4 = S, 5 = EZ, 6 = EZ + S, 7 = MZ + S, 8 = MZ + EZ, 9 = EZ + C, 10 = MZ + C, 11 = EZ + C + S, 12 = MZ + C + S, 13 = MZ + EZ + S, 14 = MZ + EZ + C (Abbreviations: C, cortex; EZ, elongation zone; MZ, meristematic zone; S, stele).

TF roles in response to hormone treatment (Clark et al., 2019; 2021; Van den Broeck et al., 2021) (See Section 2 for details). The resulting GRN consisted of 15,856 nodes (genes) with a total of 86,461 directed edges (Figure 4 and Supplemental Table S3). A circular layout visualization of the complete GRN illustrates the presence of several distinct groups (circles) based on their underlying tissue enrichment, either within a singular root region (meristematic zone, elongation zone, cortex, or stele) or between multiple combinatorial root zones based on SC-ION generated ICA clustering assignments (Supplemental Table S3).

The nodes contained within our GRN fell into one of 14 tissue enrichment groups with content sizes ranging from 2,862 nodes enriched in the cortex + stele (group 1) down to 98 nodes in the meristematic zone + elongation zone + cortex (group 14). The tissue enrichment groupings also featured varying numbers of auxin-responsive genes and a high degree of interconnectedness as evidenced by the number of edges linking nodes within a grouping. The GRN contained a total of 1,372 unique DE transcription factors thus we investigated the predicted regulatory relationships of these transcription factors and their
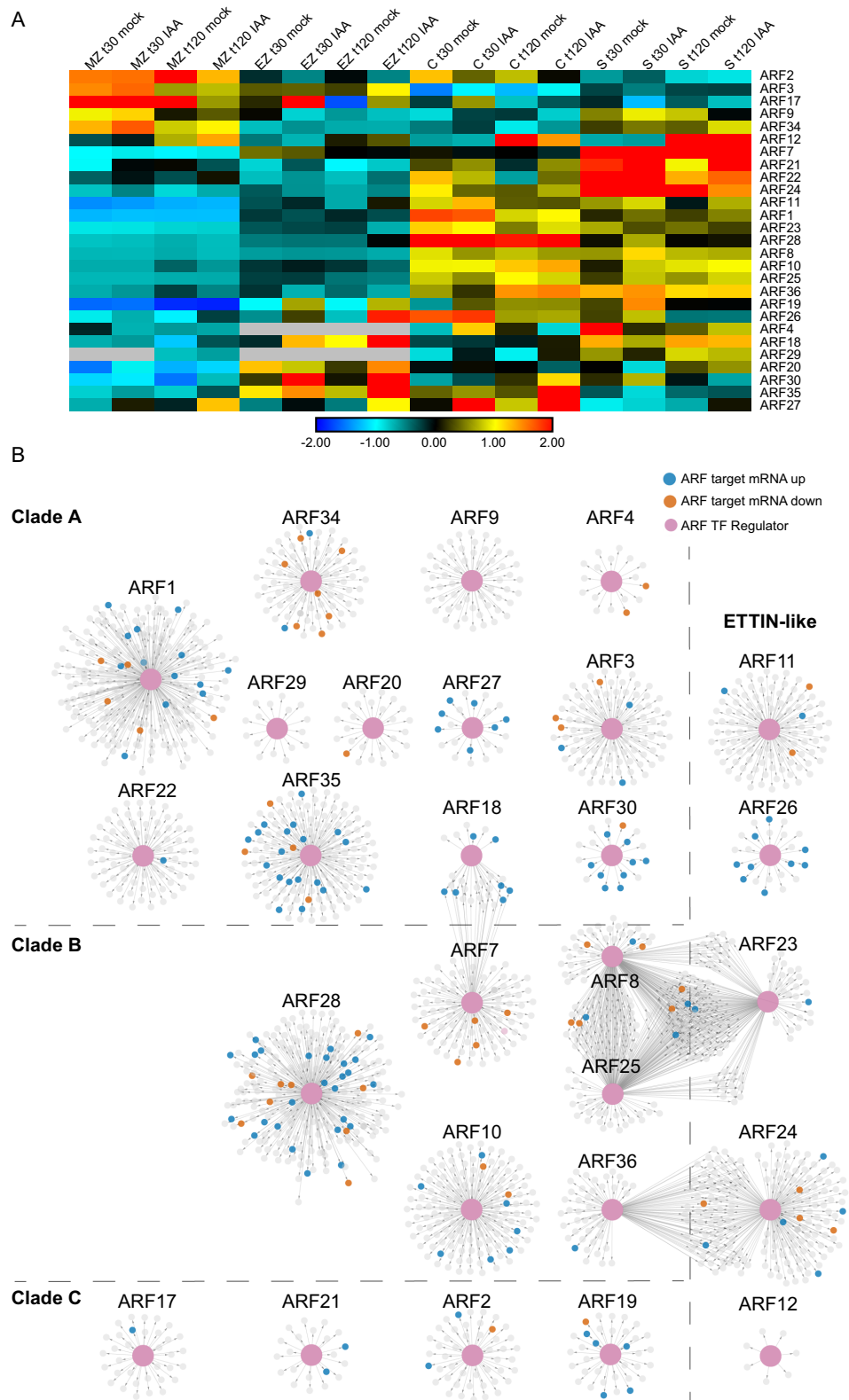
Fig. 5. Auxin-Response Factor (ARF) transcription factor gene regulatory subnetworks associated with primary maize roots. (a) ARF expression across tissues at t30 and t120 auxin treatments. (b) ARF GRN networks arranged by clade classification: Clade A, Clade B, Clade C, or ETTIN-Like. The central enlarged pink nodes within each network represent the ARF of interest labeled above the network and the connected small nodes represent that ARFs target genes. Target genes are colored according to the directionality of their transcript expression in response to auxin: grey, no significant transcript change; vermillion, decreased transcript level; blue, increased transcript level.

targets that are known to be involved in auxin signaling and maize root architecture (Figure 4 and Supplemental Table S3). Root development-associated transcription factors represented in the data include LBD-transcription factor family members and multiple members of the maize SHI/STY (SRS) family (Gomariz-Fernández et al., 2017), such as the known transcriptional activator *lateral root primordia 1* (Zm00001d011843) that is required for maize root morphogenesis (Zhang et al., 2015). In addition, a known auxin-induced transcription factor that is required for maize root development, RTCS1 (Zm00001d027679) (Tai et al., 2016; Taramino et al., 2007; Xu et al., 2015), was predicted in the GRN to regulate 57 target genes including the auxin-responsive gene AUX/IAA32 (Zm00001d018973) (Supplemental Table S3). A previous study identified putative targets of RTCS1 (also called RTCS) from embryonic transcriptional data that included cell cycle and auxin pathway genes (Tai et al., 2016). Our results provide a novel putative set of root-expressed RTCS1 targets that can support further research on this key TF.

ARF transcription factors represent a critical regulatory component of the auxin response, thus we set out to inspect their target gene relationships within the GRN at a deeper level. First, we identified all of the annotated ARFs present in the GRN and observed that 27 of the 33 expressed maize ARF family members were present in the GRN (according to the ARF nomenclature from Galli et al. (2015). For these 27 ARFs and their first node neighbor targets, we generated subnetworks that were visualized in perfuse force-directed layout in Cytoscape (Figure 5 and Supplemental Table S4). These 27 ARFs are predicted to regulate 2,067 unique target genes at either 30 or 120 min. Notably, representative ARFs from each of the four distinct evolutionary ARF clades (Galli et al., 2018) were found to be present in the GRN, including 12 clade A ARFs, 6 clade B ARFs, 4 clade C ARFs, and 5 ETTIN-like ARFs (visualized as pink nodes in Figure 5). In general, most ARFs had target nodes that were DE in response to auxin (coded blue and orange in Figure 5) and exhibit unique target genes. In three instances there are several ARFs that have shared target genes, including ARF18 and ARF7; ARF8, ARF23 and ARF25; and ARF24 and ARF36. Notably, the ARFs with shared targets span phylogenetic clades, suggesting that the properties of ARFs cannot be predicted based on sequence evolution alone. In addition, we examined the ARF target genes and found that they include auxin-related genes belonging to the *ARF* (5), *Aux/IAA* (8), *SAUR* (3), and *GRETCHEN HAGEN* (*GH3)* (1) families. Such targets are well-known types of auxin-responsive genes (Bargmann et al., 2013; Galli et al., 2018; Lewis et al., 2013; Mutte et al., 2018; Nemhauser et al., 2006) and indicate that ARF proteins are engaged in feedback loops.

In this work, we utilized a combinatorial approach of transcriptome analysis and gene network inference to identify temporally auxin-responsive genes across root tissue types. By elucidating the complex inner workings of auxin-mediated gene expression during primary maize root development we can begin to answer questions surrounding root architecture in this key crop. A molecular understanding of the dynamics of root growth can aid in informing strategies to create next-generation crops with more efficient water and nutrient uptake capabilities.

Acknowledgement

References

Anders, S., **Pyl, P. T.**, & **Huber, W.** (2015). HTSeq—A python framework to work with high-throughput sequencing data. *Bioinformatics*, **31**, 166–169. https://doi.org/10.1093/bioinformatics/btu638

Atkinson, J. A., **Rasmussen, A.**, **Traini, R.**, **Voss, U.**, **Sturrock, C.**, **Mooney, S. J.**, **Wells, D. M.**, & **Bennett, M. J.** (2014). Branching out in roots: Uncovering form, function, and regulation. *Plant Physiology*, **166**, 538–550. https://doi.org/10.1104/pp.114.245423

Bargmann, B. O. R., **Vanneste, S.**, **Krouk, G.**, **Nawy, T.**, **Efroni, I.**, **Shani, E.**, **Choe, G.**, **Friml, J.**, **Bergmann, D. C.**, **Estelle, M.**, & **Birnbaum, K. D.** (2013). A map of cell type-specific auxin responses. *Molecular Systems Biology*, **9**, 688. https://doi.org/10.1038/msb.2013.40

Bonnot, T., **Gillard, M.**, & **Nagel, D.** (2019). A simple protocol for informative visualization of enriched gene ontology terms. *Bio-Protocol*, **9**, 3429. https://doi.org/10.21769/BioProtoc.3429

Brunoud, G., **Wells, D. M.**, **Oliva, M.**, **Larrieu, A.**, **Mirabet, V.**, **Burrow, A. H.**, **Beeckman, T.**, **Kepinski, S.**, **Traas, J.**, **Bennett, M. J.**, & **Vernoux, T.** (2012). A novel sensor to map auxin response and distribution at high spatio-temporal resolution. *Nature*, **482**, 103–106. https://doi.org/10.1038/nature10791

Calderón Villalobos, L. I. A., **Lee, S.**, **De Oliveira, C.**, **Ivetac, A.**, **Brandt, W.**, **Armitage, L.**, **Sheard, L. B.**, **Tan, X.**, **Parry, G.**, **Mao, H.**, **Zheng, N.**, **Napier, R.**, **Kepinski, S.**, & **Estelle, M.** (2012). A combinatorial TIR1/AFB–Aux/IAA co-receptor system for differential sensing of auxin. *Nature Chemical Biology*, **8**, 477–485. https://doi.org/10.1038/nchembio.926

Clark, N. M., **Buckner, E.**, **Fisher, A. P.**, **Nelson, E. C.**, **Nguyen, T. T.**, **Simmons, A. R.**, **de Luis Balaguer, M. A.**, **Butler-Smith, T.**, **Sheldon, P. J.**, **Bergmann, D. C.**, **Williams, C. M.**, & **Sozzani, R.** (2019). Stem-cell-ubiquitous genes spatiotemporally coordinate division through regulation of stem-cell-specific gene networks. *Nature Communications*, **10**, 5574. https://doi.org/10.1038/s41467-019-13132-2

Clark, N. M., **Nolan, T. M.**, **Wang, P.**, **Song, G.**, **Montes, C.**, **Valentine, C. T.**, **Guo, H.**, **Sozzani, R.**, **Yin, Y.**, & **Walley, J. W.** (2021). Integrated omics networks reveal the temporal signaling events of brassinosteroid response in Arabidopsis. *Nature Communications*, **12**, 5858. https://doi.org/10.1038/s41467-021-26165-3

Conway, J. R., **Lex, A.**, & **Gehlenborg, N.** (2017). UpSetR: An R package for the visualization of intersecting sets and their properties. *Bioinformatics*, **33**, 2938–2940. https://doi.org/10.1093/bioinformatics/btx364

Dharmasiri, N., Dharmasiri, S., & Estelle, M. (2005). The F-box protein TIR1 is an auxin receptor. *Nature*, **435**, 441–445. https://doi.org/10.1038/nature03543

Dobin, A., Davis, C. A., Schlesinger, F., Drenkow, J., Zaleski, C., Jha, S., Batut, P., Chaisson, M., & Gingeras, T. R. (2013). STAR: Ultrafast universal RNA-seq aligner. *Bioinformatics*, **29**, 15–21. https://doi.org/10.1093/bioinformatics/bts635

Gallavotti, A., Long, J. A., Stanfield, S., Yang, X., Jackson, D., Vollbrecht, E., & Schmidt, R. J. (2010). The control of axillary meristem fate in the maize ramosa pathway. *Development (Cambridge, England)*, **137**, 2849–2856. https://doi.org/10.1242/dev.051748

Galli, M., Khakhar, A., Lu, Z., Chen, Z., Sen, S., Joshi, T., Nemhauser, J. L., Schmitz, R. J., & Gallavotti, A. (2018). The DNA binding landscape of the maize AUXIN RESPONSE FACTOR family. *Nature Communications*, **9**, 4526. https://doi.org/10.1038/s41467-018-06977-6

Galli, M., Liu, Q., Moss, B. L., Malcomber, S., Li, W., Gaines, C., Federici, S., Roshkovan, J., Meeley, R., Nemhauser, J. L., & Gallavotti, A. (2015). Auxin signaling modules regulate maize inflorescence architecture. *Proceedings of the National Academy of Sciences of the United States of America*, **112**, 13372–13377. https://doi.org/10.1073/pnas.1516473112

Gomariz-Fernández, A., Sánchez-Gerschon, V., Fourquin, C., & Ferrándiz, C. (2017). The role of SHI/STY/SRS genes in organ growth and carpel development is conserved in the distant eudicot species Arabidopsis thaliana and Nicotiana benthamiana. *Frontiers in Plant Science*, **8**, 814. https://doi.org/10.3389/fpls.2017.00814

Haque, S., Ahmad, J. S., Clark, N. M., Williams, C. M., & Sozzani, R. (2019). Computational prediction of gene regulatory networks in plant growth and development. *Current Opinion in Plant Biology*, **47**, 96–105. https://doi.org/10.1016/j.pbi.2018.10.005

Hochholdinger, F. (2009). The maize root system: Morphology, anatomy, and genetics. In J. L. Bennetzen & S. C. Hake (Eds.), *Handbook of maize: Its biology* (pp. 145–160). Springer. https://doi.org/10.1007/978-0-387-79418-1_8

Hochholdinger, F., Yu, P., & Marcon, C. (2018). Genetic control of root system development in maize. *Trends in Plant Science*, **23**, 79–88. https://doi.org/10.1016/j.tplants.2017.10.004

Hochholdinger, F., & Zimmermann, R. (2008). Conserved and diverse mechanisms in root development. *Current Opinion in Plant Biology*, **11**, 70–74. https://doi.org/10.1016/j.pbi.2007.10.002

Huynh-Thu, V. A., Irrthum, A., Wehenkel, L., & Geurts, P. (2010). Inferring regulatory networks from expression data using tree-based methods. *PLoS One*, **5**, 10. https://doi.org/10.1371/journal.pone.0012776

Ishikawa, H., & Evans, M. L. (1993). The role of the distal elongation zone in the response of maize roots to auxin and gravity. *Plant Physiology*, **102**, 1203–1210. https://doi.org/10.1104/pp.102.4.1203

Jiang, K., Zhu, T., Diao, Z., Huang, H., & Feldman, L. J. (2010). The maize root stem cell niche: A partnership between two sister cell populations. *Planta*, **231**, 411–424. https://doi.org/10.1007/s00425-009-1059-3

Jiao, Y., Peluso, P., Shi, J., Liang, T., Stitzer, M. C., Wang, B., Campbell, M. S., Stein, J. C., Wei, X., Chin, C.-S., Guill, K., Regulski, M., Kumari, S., Olson, A., Gent, J., Schneider, K. L., Wolfgruber, T. K., May, M. R., Springer, N. M., … Ware, D. (2017). Improved maize reference genome with single-molecule technologies. *Nature*, **546**, 524–527. https://doi.org/10.1038/nature22971

Kelley, D. R. (2018). E3 ubiquitin ligases: Key regulators of hormone signaling in plants. *Molecular and Cellular Proteomics*, **17**, 1047–1054. https://doi.org/10.1074/mcp.MR117.000476

Kepinski, S., & Leyser, O. (2004). Auxin-induced SCFTIR1-Aux/IAA interaction involves stable modification of the SCFTIR1 complex. *Proceedings of the National Academy of Sciences*, **101**, 12381–12386. https://doi.org/10.1073/pnas.0402868101

Kozlova, L. V., Nazipova, A. R., Gorshkov, O. V., Petrova, A. A., & Gorshkova, T. A. (2020). Elongating maize root: Zone-specific combinations of polysaccharides from type I and type II primary cell walls. *Scientific Reports*, **10**, 10956. https://doi.org/10.1038/s41598-020-67782-0

Lewis, D. R., Olex, A. L., Lundy, S. R., Turkett, W. H., Fetrow, J. S., & Muday, G. K. (2013). A kinetic analysis of the auxin transcriptome reveals Cell Wall remodeling proteins that modulate lateral root development in *Arabidopsis*. *The Plant Cell*, **25**, 3329–3346. https://doi.org/10.1105/tpc.113.114868

Li, H., Handsaker, B., Wysoker, A., Fennell, T., Ruan, J., Homer, N., Marth, G., Abecasis, G., Durbin, R., & 1000 Genome Project Data Processing Subgroup. (2009). The sequence alignment/map format and SAMtools. *Bioinformatics*, **25**, 2078–2079. https://doi.org/10.1093/bioinformatics/btp352

Li, J., Witten, D. M., Johnstone, I. M., & Tibshirani, R. (2012). Normalization, testing, and false discovery rate estimation for RNA-sequencing data. *Biostatistics*, **13**, 523–538. https://doi.org/10.1093/biostatistics/kxr031

Liu, Y., & von Wirén, N. (2022). Integration of nutrient and water availabilities via auxin into the root developmental program. *Current Opinion in Plant Biology*, **65**, 102117. https://doi.org/10.1016/j.pbi.2021.102117

Marcon, C., Malik, W. A., Walley, J. W., Shen, Z., Paschold, A., Smith, L. G., Piepho, H.-P., Briggs, S. P., & Hochholdinger, F. (2015). A high-resolution tissue-specific proteome and phosphoproteome atlas of maize primary roots reveals functional gradients along the root axes. *Plant Physiology*, **168**, 233–246. https://doi.org/10.1104/pp.15.00138

Marshall-Colón, A., & Kliebenstein, D. J. (2019). Plant networks as traits and hypotheses: Moving beyond description. *Trends in Plant Science*, **24**, 840–852. https://doi.org/10.1016/j.tplants.2019.06.003

Matsuyama, T., Satoh, H., Yamada, Y., & Hashimoto, T. (1999). A maize glycine-rich protein is synthesized in the lateral root cap and accumulates in the Mucilage1. *Plant Physiology*, **120**, 665–674. https://doi.org/10.1104/pp.120.3.665

Mir, R., Aranda, L. Z., Biaocchi, T., Luo, A., Sylvester, A. W., & Rasmussen, C. G. (2017). A DII domain-based auxin reporter uncovers low auxin signaling during telophase and early G1. *Plant Physiology*, **173**, 863–871. https://doi.org/10.1104/pp.16.01454

Moll, P., Ante, M., Seitz, A., & Reda, T. (2014). QuantSeq 3' mRNA sequencing for RNA quantification. *Nature Methods*, **11**, 952. https://doi.org/10.1038/nmeth.f.376

Mutte, S. K., Kato, H., Rothfels, C., Melkonian, M., Wong, G. K.-S., & Weijers, D. (2018). Origin and evolution of the nuclear auxin response system. *ELife*, **7**, e33399. https://doi.org/10.7554/eLife.33399

Nascimento, M., Silva, F. F. E., Sáfadi, T., Nascimento, A. C. C., Ferreira, T. E. M., Barroso, L. M. A., Ferreira Azevedo, C., Guimarães, S. E. F., & Serão, N. V. L. (2017). Independent component analysis (ICA) based-clustering of temporal RNA-seq data. *PLoS One*, **12**, e0181195. https://doi.org/10.1371/journal.pone.0181195

Nemhauser, J. L., Hong, F., & Chory, J. (2006). Different plant hormones regulate similar processes through largely nonoverlapping transcriptional responses. *Cell*, **126**, 467–475. https://doi.org/10.1016/j.cell.2006.05.050

Novák, O., Hényková, E., Sairanen, I., Kowalczyk, M., Pospíšil, T., & Ljung, K. (2012). Tissue-specific profiling of the *Arabidopsis thaliana* auxin metabolome: *Auxin metabolite profiling in* Arabidopsis. *The Plant Journal*, **72**, 523–536. https://doi.org/10.1111/j.1365-313X.2012.05085.x

Paschold, A., Larson, N. B., Marcon, C., Schnable, J. C., Yeh, C.-T., Lanz, C., Nettleton, D., Piepho, H.-P., Schnable, P. S., & Hochholdinger, F. (2014). Nonsyntenic genes drive highly dynamic complementation of gene expression in maize hybrids. *The Plant Cell*, **26**, 3939–3948. https://doi.org/10.1105/tpc.114.130948

Pilet, P.-E., & Saugy, M. (1985). Effect of applied and endogenous indol-3-yl-acetic acid on maize root growth. *Planta*, **164**, 254–258.

Powers, S. K., & Strader, L. C. (2020). Regulation of auxin transcriptional responses. *Developmental Dynamics*, **249**, 483–495. https://doi.org/10.1002/dvdy.139

Pu, Y., Walley, J. W., Shen, Z., Lang, M. G., Briggs, S. P., Estelle, M., & Kelley, D. R. (2019). Quantitative early auxin root proteomics identifies GAUT10, a Galacturonosyltransferase, as a novel regulator of root meristem maintenance. *Molecular & Cellular Proteomics*, **18**, 1157–1170. https://doi.org/10.1074/mcp.RA119.001378

Ravazzolo, L., Boutet-Mercey, S., Perreau, F., Forestan, C., Varotto, S., Ruperti, B., & Quaggiotti, S. (2021). Strigolactones and auxin cooperate to regulate maize root development and response to nitrate. *Plant and Cell Physiology*, **62**, 610–623. https://doi.org/10.1093/pcp/pcab014

Saleem, M., Lamkemeyer, T., Schutzenmeister, A., Madlung, J., Sakai, H., Piepho, H.-P., Nordheim, A., & Hochholdinger, F. (2010). Specification of cortical parenchyma and stele of maize primary roots by asymmetric levels of auxin, cytokinin, and cytokinin-regulated proteins. *Plant Physiology*, **152**, 4–18. https://doi.org/10.1104/pp.109.150425

Shannon, P., Markiel, A., Ozier, O., Baliga, N. S., Wang, J. T., Ramage, D., Amin, N., Schwikowski, B., & Ideker, T. (2003). Cytoscape: A software environment for integrated models of biomolecular interaction networks. *Genome Research*, **13**, 2498–2504.

Somssich, M., Khan, G. A., & Persson, S. (2016). Cell Wall heterogeneity in root development of Arabidopsis. *Frontiers in Plant Science*, **7**, 1242. https://doi.org/10.3389/fpls.2016.01242

Szemenyei, H., Hannon, M., & Long, J. A. (2008). TOPLESS mediates auxin-dependent transcriptional repression during Arabidopsis embryogenesis. *Science*, **319**, 1384–1386. https://doi.org/10.1126/science.1151461

Tai, H., Opitz, N., Lithio, A., Lu, X., Nettleton, D., & Hochholdinger, F. (2016). Non-syntenic genes drive RTCS-dependent regulation of the embryo transcriptome during formation of seminal root primordia in maize (*Zea mays* L.). *Journal of Experimental Botany*, **68**, 403–414. https://doi.org/10.1093/jxb/erw422

Taramino, G., Sauer, M., Stauffer, J. L., Multani, D., Niu, X., Sakai, H., & Hochholdinger, F. (2007). The maize (Zea mays L.) RTCS gene encodes a LOB domain protein that is a key regulator of embryonic seminal and post-embryonic shoot-borne root initiation: Map-based cloning of the maize RTCS gene. *The Plant Journal*, **50**, 649–659. https://doi.org/10.1111/j.1365-313X.2007.03075.x

Taramino, G., Sauer, M., Stauffer, J. L., Multani, D., Niu, X., Sakai, H., & Hochholdinger, F. (2007). The maize (Zea mays L.) RTCS gene encodes a LOB domain protein that is a key regulator of embryonic seminal and post-embryonic shoot-borne root initiation. *The Plant Journal*, **50**, 649–659. https://doi.org/10.1111/j.1365-313X.2007.03075.x

Truskina, J., Han, J., Chrysanthou, E., Galvan-Ampudia, C. S., Lainé, S., Brunoud, G., Macé, J., Bellows, S., Legrand, J., Bågman, A.-M., Smit, M. E., Smetana, O., Stigliani, A., Porco, S., Bennett, M. J., Mähönen, A. P., Parcy, F., Farcot, E., Roudier, F., ... Vernoux, T. (2021). A network of transcriptional repressors modulates auxin responses. *Nature*, **589**, 116–119. https://doi.org/10.1038/s41586-020-2940-2

Van den Broeck, L., Spurney, R. J., Fisher, A. P., Schwartz, M., Clark, N. M., Nguyen, T. T., Madison, I., Gobble, M., Long, T., & Sozzani, R. (2021). A hybrid model connecting regulatory interactions with stem cell divisions in the root. *Quantitative Plant Biology*, **2**, E2. https://doi.org/10.1017/qpb.2021.1

von Behrens, I., Komatsu, M., Zhang, Y., Berendzen, K. W., Niu, X., Sakai, H., Taramino, G., & Hochholdinger, F. (2011). Rootless with undetectable meristem 1 encodes a monocot-specific AUX/IAA protein that controls embryonic seminal and post-embryonic lateral root initiation in maize: AUX/IAA regulation of maize root development. *The Plant Journal*, **66**, 341–353. https://doi.org/10.1111/j.1365-313X.2011.04495.x

Walley, J. W., Kelley, D. R., Nestorova, G., Hirschberg, D. L., & Dehesh, K. (2010). Arabidopsis deadenylases AtCAF1a and AtCAF1b play overlapping and distinct roles in mediating environmental stress responses. *Plant Physiology*, **152**, 866–875. https://doi.org/10.1104/pp.109.149005

Walley, J. W., Sartor, R. C., Shen, Z., Schmitz, R. J., Wu, K. J., Urich, M. A., Nery, J. R., Smith, L. G., Schnable, J. C., Ecker, J. R., Briggs, S. P., Krouk, G., Lingeman, J., Colon, A. M., Coruzzi, G., Shasha, D., Gardner, T. S., Faith, J. J., Bar-Joseph, Z., ... Stitt, M. (2016). Integration of omic networks in a developmental atlas of maize. *Science*, **353**, 814–818. https://doi.org/10.1126/science.aag1125

Wang, Y., Sun, H., Wang, H., Yang, X., Xu, Y., Yang, Z., Xu, C., & Li, P. (2021). Integrating transcriptome, co-expression and QTL-seq analysis reveals that primary root growth in maize is regulated via flavonoid biosynthesis and auxin signal transduction. *Journal of Experimental Botany*, **72**, 4773–4795. https://doi.org/10.1093/jxb/erab177

Xing, H., Pudake, R. N., Guo, G., Xing, G., Hu, Z., Zhang, Y., Sun, Q., & Ni, Z. (2011). Genome-wide identification and expression profiling of auxin response factor (ARF) gene family in maize. *BMC Genomics*, **12**, 178. https://doi.org/10.1186/1471-2164-12-178

Xu, C., Tai, H., Saleem, M., Ludwig, Y., Majer, C., Berendzen, K. W., Nagel, K. A., Wojciechowski, T., Meeley, R. B., Taramino, G., & Hochholdinger, F. (2015). Cooperative action of the paralogous maize lateral organ boundaries (LOB) domain proteins RTCS and RTCL in shoot-borne root formation. *New Phytologist*, **207**, 1123–1133. https://doi.org/10.1111/nph.13420

Yilmaz, A., Nishiyama, M. Y., Fuentes, B. G., Souza, G. M., Janies, D., Gray, J., & Grotewold, E. (2009). GRASSIUS: A platform for comparative regulatory genomics across the grasses. *Plant Physiology*, **149**, 171–180. https://doi.org/10.1104/pp.108.128579

Zhang, Y., Behrens, I. v., Zimmermann, R., Ludwig, Y., Hey, S., & Hochholdinger, F. (2015). LATERAL ROOT PRIMORDIA 1 of maize acts as a transcriptional activator in auxin signalling downstream of the Aux/IAA gene rootless with undetectable meristem 1. *Journal of Experimental Botany*, **66**, 3855–3863. https://doi.org/10.1093/jxb/erv187

Zhang, Y., Marcon, C., Tai, H., von Behrens, I., Ludwig, Y., Hey, S., Berendzen, K. W., & Hochholdinger, F. (2016). Conserved and unique features of the homeologous maize Aux/IAA proteins ROOTLESS WITH UNDETECTABLE MERISTEM 1 and RUM1-like 1. *Journal of Experimental Botany*, **67**, 1137–1147. https://doi.org/10.1093/jxb/erv519